A Novel Trust-Region-Based Algorithm with Flexible Jacobian Updates for Expedited Optimization of High-Frequency Structures

Anna Pietrenko-Dabrowska

Faculty of Electronics, Telecommunications and Informatics, Gdansk University of Technology, 80-233 Gdansk, Poland, anna.dabrowska@pg.edu.pl

Keywords: Electromagnetic simulation-driven design, antenna design, microwave design closure, trust-region framework, Broyden update.

Abstract

Simulation-driven design closure is mandatory in the design of contemporary high-frequency components. It aims at improving the selected performance figures through adjustment of the structure's geometry (and/or material) parameters. The computational cost of this process when employing numerical optimization is often prohibitively high, which is a strong motivation for the development of more efficient methods. This is especially important in the case of complex and multi-parameter structures. In the paper, an expedited trust-region-based algorithm for electromagnetic (EM)-driven design optimization of high-frequency structures is proposed. The presented technique involves a flexible sensitivity update scheme depending on the relative design changes with respect to the trust region size, as well as a direction of the design relocation and its alignment with the coordinate system axes. This allows for performing finite-differentiation-based sensitivity updates less frequently and, consequently, brings considerable computational savings. Numerical results obtained for an ultra-wideband antenna and a microwave coupler demonstrate that the

proposed algorithm outperforms the reference procedure in terms of the number of EM simulations necessary to arrive at the optimized solution (around 50 percent). At the same time, the design quality loss is minor.

1. Introduction

The importance of numerical optimization in the design of antenna and microwave components has been steadily growing over the recent years [1], [2]. One of the fundamental components of the optimization processes in high-frequency electronics is a full-wave electromagnetic (EM) analysis. EM simulation models can deliver an adequate level of performance evaluation accuracy [3]. Furthermore, they are often the only way to ensure sufficient reliability, especially for topologically complex structures for which the existing theoretical models are highly inaccurate [4], [5]. Typically carried out as the last stage of the design process, EM-driven parameter adjustment aims at the improvement of selected performance figures, such as impedance matching, bandwidth, gain, or achieving a required power split ratio, to name just a few. Satisfying these specifications by means of conventional algorithms (either global [6] or local [7,8]) normally requires massive EM simulations. The associated computational costs may be prohibitive.

Numerous techniques for alleviating the aforementioned issue have been developed, including adjoint sensitivities [9,10] and machine learning methods [11,12]. Another example is feature-based optimization, a technique that exploits a specific structure of the system response to accelerate the optimization process by reformulating the design problem in terms of the coordinates of appropriately defined characteristic points [13]. Probably the most widespread group are surrogate-assisted methods [14]-[16], where, instead of directly optimizing a high-fidelity (fine) EM model, a cheaper representation, referred to as a surrogate model, is utilized as a prediction tool and iteratively corrected using the accumulated high-fidelity data. The surrogate models may be data-driven or physics-based ones (e.g., constructed from underlying equivalent networks). The data-driven models are versatile, however their application is limited to rather low-dimensional cases [17]. The examples include kriging [18,19], Gaussian process regression [20,21], and polynomial

response surfaces [18,22]. The physics-based models are considerably less affected by the curse of dimensionality, however, at the expense of generality. Popular techniques include space mapping [14,15,23,24], as well as response correction techniques [25,26]. Surrogate-based optimization may lead to a significant computational speedup provided that the surrogate model is significantly faster than the fine model, and the two models are sufficiently well correlated. Unfortunately, in the case of practical antenna structures and miniaturized microwave components, the only available surrogates are those derived from coarse-mesh simulations [1]. Their cost is normally substantial and their multiple evaluations cannot be neglected in the overall optimization expenses.

Regardless of whether the high-fidelity model is optimized directly or using a physics-based surrogate-assisted routine, it is the overall number of EM simulations (on either low- or high-fidelity level) that determines the cost of the parameter tuning process. In this paper, a trust-region-embedded algorithm of improved computational efficiency is proposed. The key concept of the method is a flexible management scheme for the system response Jacobian updating. It utilizes the following two criteria: (i) a relative change (with respect to the trust region size) of the parameter vector between the algorithm iterations, and (ii) the alignment of the design relocation direction with the coordinate system axes. A rank-one Broyden formula for the Jacobian update is adopted for parameters satisfying the acceptance conditions pertinent to the latter criterion. For the sake of validation, an ultra-wideband antenna and a miniaturized coupler (implemented using compact microwave resonant cells, CMRCs [10]) are considered. The numerical results obtained for these benchmark structures indicate that the proposed algorithm allows for achieving a significant optimization speedup of around 50 percent, as compared to the reference TR algorithm. At the same time, the design quality degradation is minor.

2. High-Frequency Structure Optimization with Flexible Jacobian Updates

This section recalls the design optimization problem and briefly describes the reference trust-region-based algorithm. Subsequently, a detailed formulation of the proposed algorithm with a flexible Jacobian update scheme is presented, in which two separate acceleration mechanisms are combined, both aiming at the reduction of the optimization cost.

2.1. Design Closure as an Optimization Task

Here, a design closure is considered, i.e., the adjustment of (typically) geometry parameter vector $\boldsymbol{x}$ in order to improve the selected performance figures. We will denote as $\boldsymbol{R}(\boldsymbol{x})$ the response of an EM-simulated model of the structure at hand; typically, it is a frequency characteristic, e.g., scattering parameters, gain, radiation pattern, power split ratio. The task of finding the optimum design $\boldsymbol{x}^*$ can be formulated as

$$\boldsymbol{x}^* = \arg\min_{\boldsymbol{x}} U\left(\boldsymbol{R}(\boldsymbol{x})\right) \tag{1}$$

In (1), a scalar objective function U incorporates the performance specifications. Its definition depends on the type of the optimized structure. Below, two different objective functions are exemplified, further used for handling the verification cases of Section 3.

In the case of antennas, one of typical objectives is to minimize the reflection response S_{11} (which is equivalent to reducing the return loss) within the frequency range of interest F

$$U(\boldsymbol{R}(\boldsymbol{x})) = \max_{f \in F} |S_{11}(\boldsymbol{x}, f)| \tag{2}$$

In (2), the explicit dependence of $|S_{11}(\boldsymbol{x},f)|$ on both the geometry parameters $\boldsymbol{x}$ and the frequency f is shown. The optimization problem (1) with the objective function defined by (2) is formulated in a minimax sense.

If, however, multiple performance figures are to be handled, one of possible approaches is to select the main objective and control others in an implicit manner, i.e., by

casting them into constraints (e.g., using penalty functions). In the case of microwave couplers, a practical design problem may be to maximize the bandwidth *BW* (typically, symmetric with respect to the operating frequency f_0), or to obtain the assumed (either equal or non-equal) power split $d_S = |S_{21}| - |S_{31}|$ at f_0. Another objective may involve the allocation of the minima of the matching and isolation characteristics ($|S_{11}|$ and $|S_{41}|$) close to f_0. The objective function *U* comprising all of these objectives may be defined as

$$U(\boldsymbol{R}(\boldsymbol{x})) = -BW(\boldsymbol{x}) + \sigma_1 d_S(\boldsymbol{x})^2 + \sigma_2(f_{\min.S_{11}}(\boldsymbol{x}) - f_0)^2 + \sigma_3(f_{\min.S_{41}}(\boldsymbol{x}) - f_0)^2 \qquad (3)$$

In (3), $f_{\min.S11}$ and $f_{\min.S41}$ refer to the frequencies of the minima of $|S_{11}|$ and $|S_{41}|$, respectively, whereas σ_k , k = 1, 2, 3, denote the penalty coefficients. The presented penalty function concept (cf. (3)) allows for efficient handling of the expensive constraints, particularly if both the objective function and the constraints come from EM simulation [27], [28].

2.2. Trust-Region Gradient Search as a Reference Algorithm

In this paper, a standard trust-region (TR)-based gradient-search procedure [29] serves as a reference algorithm. It is an iterative routine, which generates a sequence of approximations $\boldsymbol{x}^{(i)}$, i = 0, 1, …, to the optimum design $\boldsymbol{x}^*$

$$\boldsymbol{x}^{(i+1)} = \arg \min_{x_k;\, -d^{(i)}{}_k \le x_k - x^{(i)}{}_k \le\ d^{(i)}{}_k;\, k=1,\ldots,n} U(\boldsymbol{L}^{(i)}(\boldsymbol{x})) \qquad (4)$$

where n is a number of the design variables. In (4), $\boldsymbol{L}^{(i)}(\boldsymbol{x}) = \boldsymbol{R}(\boldsymbol{x}^{(i)}) + \boldsymbol{J}_{\boldsymbol{R}}(\boldsymbol{x}^{(i)})\cdot(\boldsymbol{x} - \boldsymbol{x}^{(i)})$ is a linear approximation of $\boldsymbol{R}$ at the current iteration $\boldsymbol{x}^{(i)}$. The parameter ranges of antennas and microwave components usually differ substantially: starting from fractions of millimeters (as it is in the case of line widths or spacings) and reaching up to tens of millimeters (in the case of lengths of the transmission line). Therefore, instead of an Euclidean norm with a scalar TR radius, here, an interval type TR is adopted, determined by the size vector $\boldsymbol{d}^{(i)}$. In (4), for each component x_k of the parameter vector $\boldsymbol{x}$ the respective interval is given as: $-d^{(i)}{}_k \le x_k - x^{(i)}{}_k \le d^{(i)}{}_k$, k = 1, …, n. The initial size vector $\boldsymbol{d}^{(0)}$ is made proportional to the design space sizes,

which allows for an appropriate handling of variables of essentially different ranges. In the TR algorithm, the vector $\boldsymbol{d}^{(i)}$ is altered according to the standard rules based on the gain ratio [29]. The gain ratio is defined as $\rho = [U(\boldsymbol{R}(\boldsymbol{x}^{(i+1)})) - U(\boldsymbol{R}(\boldsymbol{x}^{(i)}))]/[U(\boldsymbol{L}^{(i)}(\boldsymbol{x}^{(i+1)})) - U(\boldsymbol{L}^{(i)}(\boldsymbol{x}^{(i)}))]$, i.e., it is an actual versus linear-model predicted objective function improvement. A positive value of the gain ratio indicates that the iteration was successful, and then the candidate design obtained by (4) is accepted.

In the design of high-frequency structures, the Jacobian $\boldsymbol{J_R}$ is usually evaluated using finite differentiation (FD), which requires performing n additional EM analyses upon each successful algorithm iteration. The computational cost of the optimization process is mainly determined by the cost of Jacobian updates. In the case of an unsuccessful iteration (i.e., $\rho < 0$), a new candidate design has to be sought by solving (4) with a reduced $\boldsymbol{d}^{(i)}$ [29], which increases the overall optimization cost by additional n EM simulations.

2.3. Enhanced Algorithm with Flexible Jacobian Updates

The high computational cost of design optimization with the conventional TR algorithm is mainly incurred by evaluating the system response Jacobian through FD. The proposed algorithm with flexible Jacobian updates delivers an effective method of alleviating this computational overhead. A significant reduction of the overall number of FD calculations needed by the algorithm to converge is achieved with the use of two independent procedures. The first routine exploits relative design changes with respect to the trust region size in order to omit the FD calculation for the selected variables; the routine is referred to as accelerated update procedure (AUP). The second one, Broyden update procedure (BUP), utilizes a direction of the design relocation, and its alignment with the coordinate system axes, as a guide for pinpointing the parameters, for which Broyden updating formula is to be utilized instead of FD. The two procedures are subsequently combined, which allows achieving

substantial cost savings, and, at the same time, the sufficient design quality, as shown in Section 3.

2.4 Selection Matrix Updating Procedure

In the proposed algorithm, a binary selection matrix $\boldsymbol{\Gamma}$ is utilized to store the information pertaining to FD calculation of Jacobian $\boldsymbol{J_R}$: if it is compulsory, the respective matrix entry equals one, otherwise it is set to zero. In the first iteration, the selection matrix $\boldsymbol{\Gamma}$ is initialized as an $n \times 1$ column vector: $\gamma_{k.1} = 1$, $k = 1, \ldots, n$. Thus, the entire Jacobian $\boldsymbol{J_R}$ is estimated with FD at the beginning of the optimization process. Next, in each iteration, the matrix $\boldsymbol{\Gamma}$ is accrued by an extra column that contains the information regulating the Jacobian update in the upcoming iteration.

In the following, a detailed description of both update procedures: the accelerated (AUP) and the Broyden (BUP) update procedure is provided. The former selects the parameters that exhibit small relative changes between iterations, the latter seeks for the parameters characterized by a good alignment of the most current design relocation vector with the corresponding coordinate system basis vectors. For the identified parameters, the calculation of the respective part of the Jacobian is either skipped (AUP) or superseded with the Broyden formula (BUP). The outcomes of both procedures are then combined in order to create the selection matrix $\boldsymbol{\Gamma}$. Both procedures are presented in the form of the flow diagram in Fig. 1.

Accelerated Update Procedure. In the AUP procedure (see Panel A of Fig. 1), the changes of the geometry parameters throughout the optimization course are monitored. The adopted measure is defined as a relative design change of the k-th parameter, $k = 1, \ldots, n$, w.r.t. the TR region size in the i-th iteration,

$$\alpha_k^{(i+1)} = \left| x_k^{(i+1)} - x_k^{(i)} \right| \Big/ d_k^{(i)} \quad k = 1, \ldots, n, \tag{5}$$

In (5), $x_k^{(i)}$, $x_k^{(i+1)}$ and $d_k^{(i)}$ denote the k-th components of vectors $\boldsymbol{x}^{(i)}$, $\boldsymbol{x}^{(i+1)}$, and $\boldsymbol{d}^{(i)}$, respectively. In addition, $\boldsymbol{J}_k$ refers to the k-th column of the Jacobian $\boldsymbol{J}_{\boldsymbol{R}}$ (associated with the kth parameter of the structure under design). The decision about the update of $\boldsymbol{J}_k$ through FD in the (i+1)th iteration is based on: (i) the decision factor $\alpha_k^{(i+1)}$ and (ii) monitoring of the optimization history run (this is to ensure that $\boldsymbol{J}_k$ is estimated through FD at least once per N iterations).

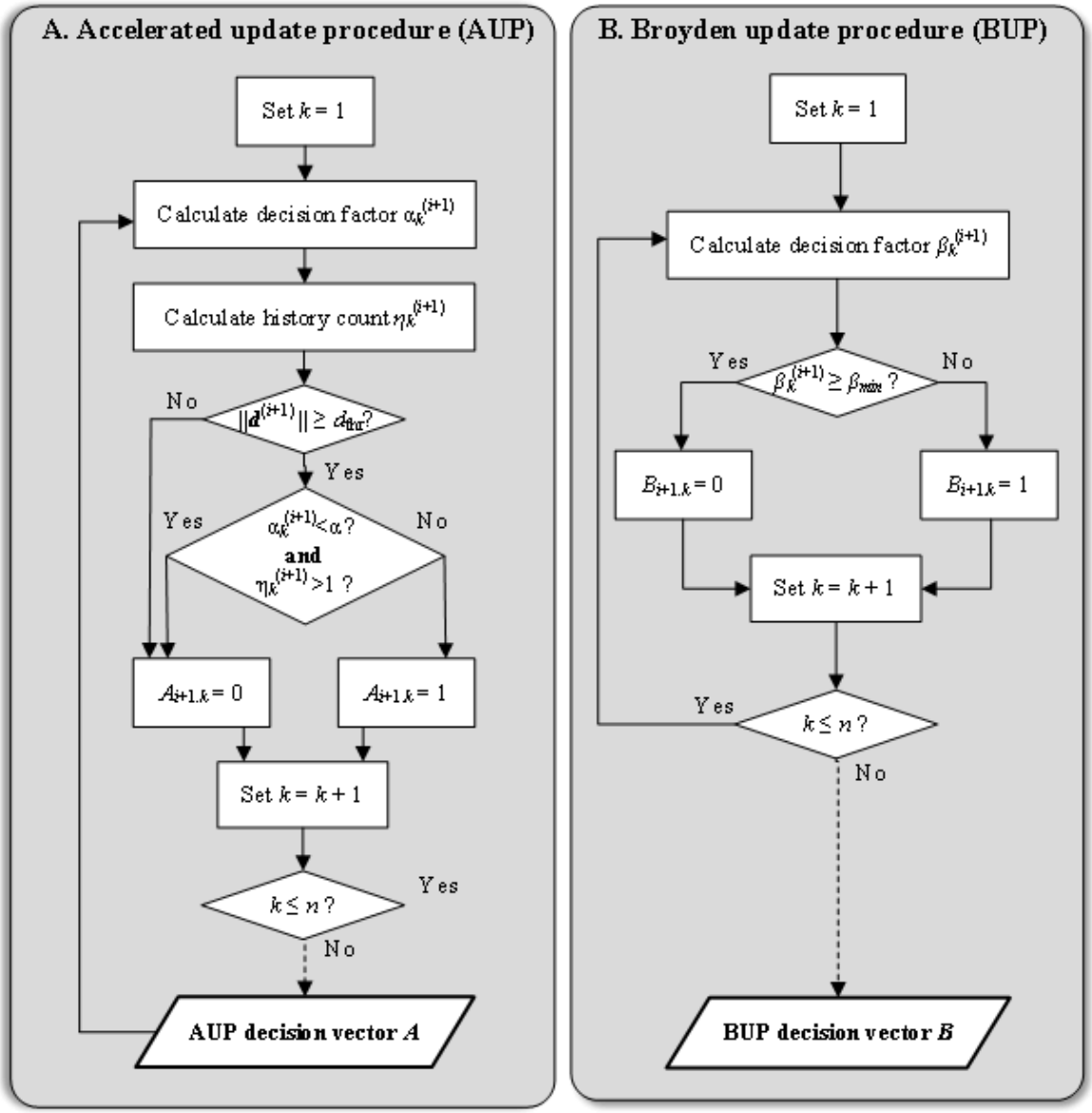

Fig. 1. Flow diagram of the update procedures: accelerated update procedure (A) and Broyden update procedure (B). The following notation is used: (i) AUP parameters: $\alpha_k^{(i+1)}$ – a decision factor for k-th geometry parameter and (i+1)th iteration; $\eta_k^{(i+1)}$ – a history count, α – threshold value, $\boldsymbol{A}$ – an AUP binary decision vector; (ii) BUP parameters: $\beta_k^{(i+1)}$ – a decision factor for k-th geometry parameter and (i+1)th iteration, $\beta_{\min}$ – an alignment threshold value, $\boldsymbol{B}$ – a BUP binary decision vector.

The optimization history is scrutinized at the span of the preceding N iterations (N is the algorithm control parameter). The history count $\eta_k^{(i+1)}$ is defined as the total number of iterations (among the last N iterations), in which FD was performed for the k-th parameter. The outcome of the AUP procedure—the binary AUP decision vector $\boldsymbol{A}$—is a result of the conversion of $\alpha_k^{(i+1)}$ and $\eta_k^{(i+1)}$. The following notation is used: $A_{i+1.k}$ is the k-th entry of the vector $\boldsymbol{A}$, pertaining to the (i+1)th iteration. If $A_{i+1.k} = 1$, the estimation of $\boldsymbol{J}_k$ through FD is recommended; otherwise (i.e., $A_{i+1.k} = 0$) it can be omitted.

The algorithm control parameter N allows for controlling the trade-offs between computational speedup and the design quality. The higher the value of N, the higher the savings, however at the expense of deteriorated design quality, as increasing N leads to lengthening the span of iterations, during which Jacobian update through FD is not omitted. On the other hand, too small N may lead to a substantially prolonged optimization time, compared even to that of the conventional TR algorithm.

The vector $\boldsymbol{A}$ is created as follows. First, the decision factors $\alpha_k^{(i+1)}$, $k = 1, \ldots, n$, (cf. (5)) and the history counts $\eta_k^{(i+1)}$ are assessed for all parameters. Next, $A_{i+1.k}$ is assigned a zero value in the two following cases:

1. For all parameters: if the TR size $\|\boldsymbol{d}^{(i)}\|$ does not exceed a user-specified threshold d_{thr},
2. For the selected parameters: if the TR size $\|\boldsymbol{d}^{(i)}\|$ is over the threshold d_{thr}, and if both: (i) $\boldsymbol{J}_k$ was calculated with FD at least once in the last N iterations (i.e., $\eta_k^{(i+1)} > 1$), and (ii) $\alpha_k^{(i+1)}$ is below the user-specified threshold α.

Broyden Update Procedure. In the BUP procedure (see Panel B of Fig. 1), the parameters for which the respective columns of $\boldsymbol{J_R}$ can (potentially) be calculated using the rank-one Broyden update formula (BF) instead of FD are determined. The BF update is implemented as

$$\boldsymbol{J}_{\boldsymbol{R}}^{(i+1)} = \boldsymbol{J}_{\boldsymbol{R}}^{(i)} + \frac{\left(\boldsymbol{f}^{(i+1)} - \boldsymbol{J}_{\boldsymbol{R}}^{(i)} \cdot \boldsymbol{h}^{(i+1)}\right) \cdot \boldsymbol{h}^{(i+1)T}}{\boldsymbol{h}^{(i+1)T} \boldsymbol{h}^{(i+1)}}, \qquad i = 0, 1, \ldots \tag{6}$$

In (6), $\boldsymbol{f}^{(i+1)} = \boldsymbol{R}(\boldsymbol{x}^{(i+1)}) - \boldsymbol{R}(\boldsymbol{x}^{(i)})$, and $\boldsymbol{h}^{(i+1)} = \boldsymbol{x}^{(i+1)} - \boldsymbol{x}^{(i)}$. It is worth mentioning that the Jacobian estimate $\boldsymbol{J}_{\boldsymbol{R}}^{(i)}$ (calculated after performing i iterations) incorporates information about the system response sensitivity merely in an i-dimensional subspace spanned by the vectors $\boldsymbol{h}^{(1)}$, $\boldsymbol{h}^{(2)}$, …, $\boldsymbol{h}^{(i)}$. In consequence, in the spaces of higher dimensions, usually poor results are obtained with the sole use of BF.

BUP is governed by a vector B created as follows. First, the alignment factors $\beta_k^{(i+1)} = |\boldsymbol{h}^{(i+1)T}\boldsymbol{e}^{(k)}|/\|\boldsymbol{h}^{(i+1)}\|$ are calculated for each parameter k, where $\boldsymbol{e}^{(k)} = [0 \ \ldots \ 0 \ 1 \ 0 \ \ldots \ 0]^T$ is the standard basis vector. Note that $0 \le \beta_k^{(i+1)} \le 1$ ($\beta_k^{(i+1)} = 0$ and $\beta_k^{(i+1)} = 1$ for $\boldsymbol{h}^{(i+1)}$ and $\boldsymbol{e}^{(k)}$ being orthogonal, and collinear, respectively). If $\beta_k^{(i+1)} > \beta_{\min}$ (the user-defined acceptance threshold), the corresponding component $B_{i+1,k}$ of the vector $\boldsymbol{B}$ is assigned 0; otherwise, $B_{i+1,k} = 1$. Higher values of $\beta_{\min}$ create stricter conditions for using BF and possibly bring lower computational savings accompanied with the higher expected design quality.

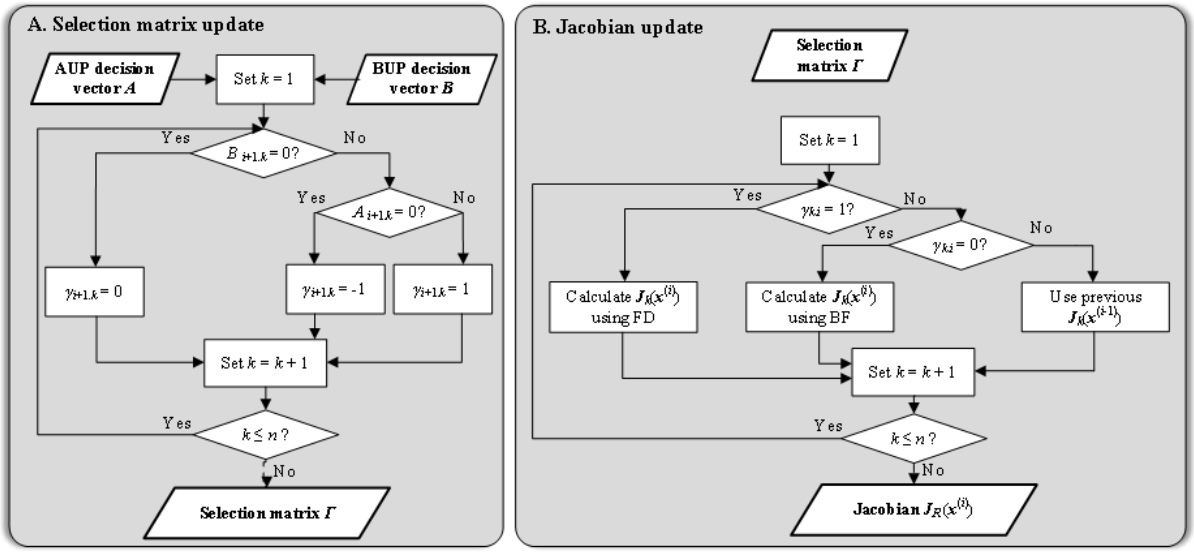

Fig. 2. Flow diagram of the selection matrix $\boldsymbol{\Gamma}$ update procedure (A) and resulting Jacobian update procedure (B); for the details on the AUP and BUP decision vectors see Fig. 1.

Jacobian Update. Both the AUP and BUP contribute to the construction of the matrix $\boldsymbol{\Gamma}$ mentioned at the beginning of Section 2.4. The construction process is shown graphically in Panel A of Fig. 2, whereas the flow of the Jacobian update procedure is presented in Panel B. As stated above, $\boldsymbol{\Gamma}$ is expanded by an additional column in each iteration, which is derived as

follows. For a given parameter k, the entry $\gamma_{i+1,k}$ of matrix $\boldsymbol{\Gamma}$ is set to 0, if $B_{i+1.k} = 0$ (irrespectively of $A_{i+1.k}$), and in that case $\boldsymbol{J}_k$ is calculated with BF. On the other hand, if $B_{i+1.k} = 1$ and $A_{i+1.k} = 0$, then $\gamma_{i+1,k}$ is assigned –1, indicating the usage of $\boldsymbol{J}_k$ from the previous iteration, i.e., $\boldsymbol{J}_k(\boldsymbol{x}^{(i+1)}) = \boldsymbol{J}_k(\boldsymbol{x}^{(i)})$. In the case of $B_{i+1.k} = A_{i+1.k} = 1$, $\boldsymbol{J}_k$ is estimated through FD (as both procedures indicate it is obligatory). The numerical results of Section 3 indicate substantial computational savings that can be obtained this way.

3. Numerical validation

A benchmark set comprises two high-frequency structures: a wideband antenna [30] shown in Fig. 3(a) and an equal-split rat-race coupler (RRC) [31] presented in Fig. 3(b). The antenna is implemented on Taconic RF-35 substrate (h = 0.762 mm, ε_r = 3.5, tanδ = 0.0018). It utilizes a quasi-circular radiator and a modified ground plane for bandwidth enhancement. The design variables are $\boldsymbol{x} = [L_0\ dR\ R\ r_{rel}\ dL\ dw\ L_g\ L_1\ R_1\ dr\ c_{rel}]^T$. The lower and upper bounds for design variables are: $\boldsymbol{l} = [0.2\ 2\ 0.2\ 0.5\ 0.2]^T$ and $\boldsymbol{u}=[1\ 8\ 1\ 5.5\ 1]^T$; all dimensions in mm. The antenna is to be optimized for minimum reflection within the UWB frequency range (3.1 GHz to 10.6 GHz).

The second structure (RRC) is also implemented on RF-35 substrate and its independent geometry parameters are $\boldsymbol{x} = [w_1\ l_1\ w_2\ l_2\ w_3]^T$, whereas $l_3 = 19w_1 + 18w_2 + w_3 – l_1$, $l_4 = 5w_1 + 6w_2 + l_2 + w_3$, $l_5 = 3w_1 + 4w_2$ and $w_4 = 9w_1 + 8w_2$ (all in mm) are relative dimensions. The lower and upper bounds for the parameters are the following: $\boldsymbol{l} = [4\ 0\ 3\ 0.1\ 0\ 0\ 4\ 0\ 2\ 0.2\ 0.2]^T$ and $\boldsymbol{u} = [15\ 6\ 8\ 0.9\ 5\ 8\ 15\ 6\ 5\ 1.0\ 0.9]^T$, respectively (dimensions in mm). The coupler is to be optimized for maximum bandwidth (defined at –20 dB level of matching and isolation and symmetric around f_0). The RRC is supposed to operate at f_0 = 1 GHz. The computational models are implemented in CST Microwave Studio.

For the sake of adequate assessment of the optimization process performance, the tested algorithms were executed (for each structure) ten times with random initial designs.

Table 1 contains the statistics, including the results obtained with the reference TR algorithm (see Section 2.2). The representative plots of the initial and the optimized responses for the antenna and the RRC are shown in Fig. 4. In the case of AUP, the control parameter value N = 3 was adopted, as this value ensures good design quality while retaining substantial cost savings (the quality versus speedup trade-off determined by different values of N is investigated in depth in [32]). Several values of the alignment algorithm control parameter (BUP) were used for each structure and for each initial design: β_0 = 0, 0.025, 0.05, 0.1, 0.2 and 0.3.

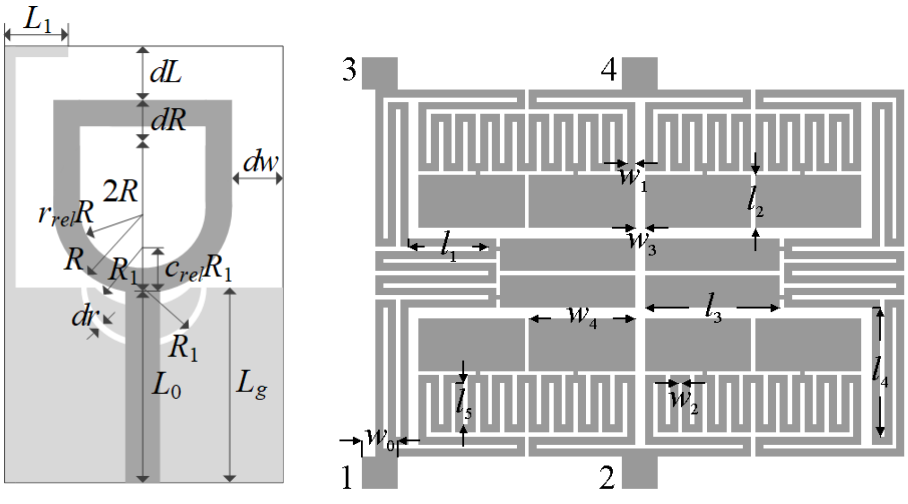

Fig. 3. High-frequency structures used for benchmark purposes: (a) UWB antenna of [30], and (b) CMRC-based miniaturized microstrip rat-race coupler of [31].

Note that increasing the threshold value leads to lower computational savings, because the condition for applying the Broyden update formula becomes more rigorous (and, consequently, FD is performed more frequently). Still, the highest value of the alignment acceptance threshold (i.e., β_0 = 0.3), bringing the best design quality, delivers a satisfactory reduction of the overall optimization cost (57% for the antenna and 48% for the RRC). Table 1 also includes the case of β_0 = 0, corresponding to the Jacobian updated exclusively with the use of BF. This is to demonstrate that abstaining from FD produces designs of an insufficient quality. Here, the standard deviation of the respective objective functions calculated for the set of

performed algorithm runs is used for the result repeatability quantification. For all the values of the acceptance threshold (except for β_0 = 0), the standard deviation value is nearly the same, which is an advantage of the proposed algorithm. In addition, the values of both objective functions: maximum in-band reflection S_{11} (antenna) and the bandwidth *BW* (RRC) are nearly constant, irrespective of the threshold value changes.

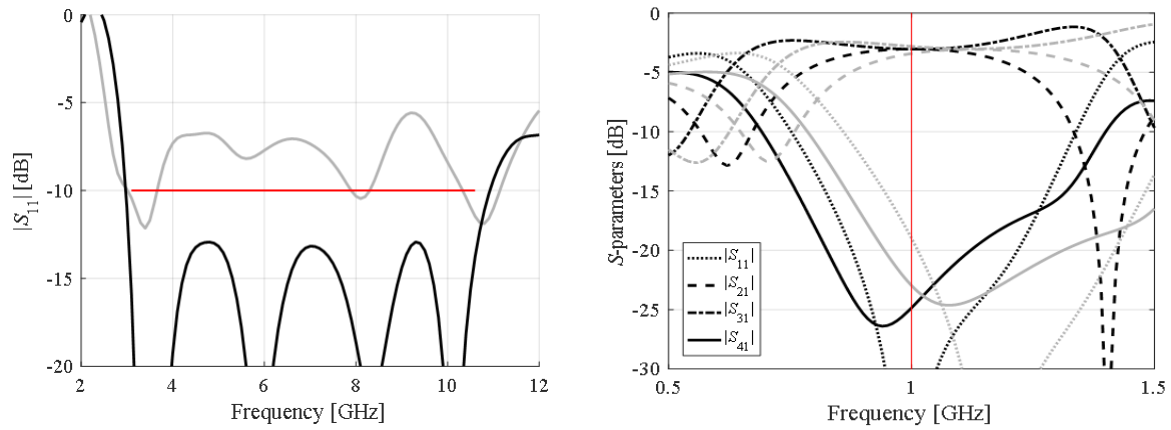

Fig. 4. Representative reflection responses of the considered high-frequency components: (a) wideband antenna (the horizontal line indicates the design specifications), (b) compact RRC (the vertical line indicates the required operating frequency f_0). The initial and optimized design are marked gray and black, respectively.

The optimum threshold value for the antenna appears to be β_0 = 0.1, because it secures computational savings as high as 61%. At the same time, the design quality degrades to a small extent, and this is also the case for the standard deviation. On the other hand, for the coupler, the most advantageous setup seems to be β_0 = 0.05. It delivers the cost savings of around 53%, as well as the best bandwidth accompanied by the smallest bandwidth standard deviation.

Table 2 provides the results obtained by means of the AUP and BUP procedures used separately. This data is given to emphasize the benefits of combining both methods into one framework. As far as the AUP procedure is concerned, the sole usage of it in the case of the antenna, ensures the design quality and the cost savings almost equal to those obtained with BUP at β_0 = 0.1. While the combined procedures yield nearly the same solution quality, the cost savings are higher (around 61 percent for the combined version versus approx.

47 percent for either AUP or BUP). Whereas for the coupler, employing only the AUP procedure delivers the same bandwidth as with β_0 = 0.05, accompanied by lower savings (around percent for AUP and almost 69percent for BUP) and higher standard deviation (nearly equal to that obtained for β_0 = 0). The combined procedures, however, lead to a better bandwidth, along with the savings of around 53 percent and the same standard deviation as for AUP.

It can be concluded from the comparison of the results of Tables 1 and 2, that it is the combination of the two procedures that allows for making the quality of the solution almost independent of β_0. Clearly, the increase in β_0 for the BUP procedure only, leads to an improvement of the quality of the solution, both in terms of the objective function value and the standard deviation. However, this comes at the expense of significantly lowered cost savings. As a matter of fact, the savings for BUP are considerably smaller than for the combined algorithm: they drop to around 20 percent for the antenna, and to barely 4 percent for the RRC. The algorithm involving both procedures permits obtaining the designs of a quality comparable to BUP, however, associated with significantly higher computational savings.

4. Conclusions

The paper proposes a novel procedure for a cost-efficient design optimization of high-frequency structures. It is based on the standard trust-region gradient-based algorithm with numerical derivatives, enhanced by a flexible Jacobian updating scheme. The proposed algorithm involves two separate acceleration mechanisms: (i) replacing the cost-inefficient finite differentiation with Broyden updates, and (ii) suppressing sensitivity updates altogether for the selected parameters. Identification of relevant parameters is based on the analysis of design relocation between the algorithm iterations. The proposed algorithm delivers significant computational savings associated with only minor

degradation of the design quality, which has been demonstrated for a wideband antenna and a miniaturized microstrip coupler. The future work will include application of the algorithm within surrogate-based optimization frameworks.

Acknowledgement

This work is partially supported by National Science Centre of Poland Grant 2015/17/B/ST6/01857.

REFERENCES

1. Koziel S, Ogurtsov S. *Antenna design by simulation-driven optimization. Surrogate-based approach*. New York: Springer; 2014.
2. Zhang J, Zhang C, Feng F, Zhang W, Ma J, Zhang QJ. Polynomial chaos-based approach to yield-driven EM optimization. *IEEE Trans Microwave Theory Tech*. 2018; 66(7): 3186–3199.
3. Sevgi L. *Electromagnetic modeling and simulation*. IEEE Press Series on Electromagnetic Wave Theory; 2014.
4. Koziel S, Bekasiewicz A. *Multi-objective design of antennas using surrogate models*. Singapur: World Scientific; 2016.
5. Koziel S, Kurgan P. Compact cell topology selection for size-reduction-oriented design of microstrip rat-race couplers. *Int J RF Microwave Comput Aided Eng*. 2018; 28(5).
6. Nocedal J, Wright SJ. *Numerical Optimization*. 2nd ed. New York: Springer; 2006.
7. Lalbakhsh A, Afzal MU, Esselle KP. Multiobjective particle swarm optimization to design a time-delay equalizer metasurface for an electromagnetic band-gap resonator antenna. *IEEE Antennas Wirel Propag Lett*. 2017; 16: 915–915.

8. Darvish A, Ebrahimzadeh A. Improved fruit-fly optimization algorithm and its applications in antenna array synthesis. *IEEE Trans Antennas Propag*. 2018; 66(4):1756-1766.
9. Joshi D, Dash S, Jatana HS, Bhattacharjee R, Trivedi G. Analog circuit optimization using adjoint network based sensitivity analysis. *AEU - Int J Electr Comm*. 2017, 82:221-225.
10. Koziel S, Bekasiewicz A. Rapid design optimization of antennas using variable-fidelity EM models and adjoint sensitivities. *Eng Comput*, 2016;33(7):2007–2018.
11. Xiao LY, Shao W, Ding X, Wang BZ. Dynamic adjustment kernel extreme learning machine for microwave component design. *IEEE Trans Microwave Theory Tech*. 2018;66(10):4452–4461.
12. Fu H, Vong C-M, Wong P-K, Yang Z. Fast detection of impact location using kernel extreme learning machine. *Neural Comput Applicat*. 2016; 27(1):121–130.
13. Koziel S. Fast simulation-driven antenna design using response-feature surrogates. *Int J RF Microwave Comput Aided Eng*. 2015;25(5):394-402.
14. Baratta IA, de Andrade CB, de Assis RR, Silva EJ. Infinitesimal dipole model using space mapping optimization for antenna placement. *IEEE Antennas Wirel Propag Lett*. 2018;17(1):17-20.
15. Xu J, Li M, Chen R. Space mapping optimisation of 2D array elements arrangement to reduce the radar cross-scattering. *IET Microw Antennas Propag*. 2017; 11(11):1578-1582.
16. Xu J, Li M, Chen R. Lump-loaded antenna optimization by manifold mapping algorithm with method of moments. *Eng Analysis Boundary Elem*. 2018; 89:45-49.

17. de Villiers DIL, Couckuyt I, Dhaene T. Multi-objective optimization of reflector antennas using kriging and probability of improvement. *IEEE Int Symp Ant Prop.* 2017:985-986.
18. Chávez-Hurtado JL, Rayas-Sánchez JE. Polynomial-based surrogate modeling of RF and microwave circuits in frequency domain exploiting the multinomial theorem. *IEEE Trans Microwave Theory Tech*. 2016; 64(12):4371-4381.
19. Hassan SO, Etman AS, Soliman EA. Optimization of a novel nano antenna with two radiation modes using kriging surrogate models. *IEEE Photonics Journal*. 2018;10(4):1-17.
20. Jacobs JP. Characterization by Gaussian processes of finite substrate size effects on gain patterns of microstrip antennas. *IET Microw Antennas Propag*. 2016;10(11): 1189–1195.
21. Jacobs JP, Koziel S. Two-stage framework for efficient Gaussian process modeling of antenna input characteristics. *IEEE Trans Antennas Propag*. 2014; 62(2):706-713.
22. Barmuta P, Ferranti F, Gibiino GP, Lewandowski A, Schreurs DMM. Compact behavioral models of nonlinear active devices using response surface methodology. *IEEE Trans Microwave Theory Tech*. 2015; 63(1):56-64.
23. Bandler JW, Cheng QS, Dakroury SA, Mohamed AS, Bakr MH, Madsen K, Sondergaard J. Space mapping: the state of the art. *IEEE Trans Microwave Theory Tech*. 2004; 52(1):337-361.
24. Simsek M. Aoad A. Multiple operating frequency selections for reconfigurable antenna design by SM based optimization *IET Microw Antennas Propag*. 2017; 11(13):1898-1908.
25. Koziel S, Leifsson L. *Simulation-driven design by knowledge-based response correction techniques*. New York: Springer; 2016.

26. Su Y, Lin J, Fan Z, Chen R. Shaping optimization of double reflector antenna based on manifold mapping. *Int Applied Comput Electromagn Society Symp (ACES)*. 2017.
27. Koziel S, Kurgan P. Compact cell topology selection for size-reduction-oriented design of microstrip rat-race couplers. *Int J RF Microwave Comput Aided Eng*. 2018;28(5).
28. Koziel S, Kurgan P. Inverse modeling for fast design optimization of small-size rat-race couplers incorporating compact cells. *Int J RF Microwave Comput Aided Eng*. 2018;28(5).
29. Conn AR, Gould NIM, Toint PL. *Trust Region Methods*. MPS-SIAM Series on Optimization; 2000.
30. Alsath MGN, Kanagasabai M. Compact UWB monopole antenna for automotive communications. *IEEE Trans Antennas Propag*. 2015;63(9):4204-4208.
31. Koziel S, Bekasiewicz A, Kurgan P. Rapid design and size reduction of microwave couplers using variable-fidelity EM-driven optimization. *Int J RF Microwave Comput Aided Eng*. 2016;26(1):27-35.
32. Koziel S, Pietrenko-Dabrowska A. An efficient trust-region algorithm for wideband antenna optimization, European Antennas and Propagation Conference, Krakow, Poland, 2019.

Table 1 Performance Statistics of the Proposed Algorithm for the Structures of Fig. 3.

Algorithm		UWB Antenna				Compact RRC			
		Cost[1]	Cost savings[2] [%]	Max $\|S_{11}\|$[3] [dB]	SD (max$\|S_{11}\|$)[4] [dB]	Cost[1]	Cost savings[2] [%]	BW[5] [GHz]	SD(BW)[6] [GHz]
Reference		111.2	–	−14.9	0.6	43.0	–	0.27	0.01
β_0	0[$]	27.4	75.4	−13.3	1.3	15.9	63.0	0.17	0.12
	0.025	31.0	72.1	−13.4	1.2	17.4	59.5	0.19	0.10
	0.05	35.5	68.1	−13.5	1.2	20.3	52.8	0.22	0.10
	0.1	43.0	61.3	−13.6	1.2	22.0	48.8	0.19	0.11
	0.2	51.1	54.0	−13.6	1.2	22.6	47.4	0.20	0.11
	0.3	47.4	57.1	−13.4	1.0	22.4	47.9	0.20	0.11

[1] Number of EM simulations averaged over 10 algorithm runs (random initial points);
[2] Percentage-wise cost savings w.r.t. the reference algorithm;
[3] Objective function values for the UWB antenna (maximum in-band reflection S_{11} in dB);
[4] Standard deviation of S_{11} in dB across 10 algorithm runs;
[5] Objective function values for the compact RRC (bandwidth BW in GHz);
[6] Standard deviation of BW in dB across 10 algorithm runs;
[$] Broyden-only Jacobian updates meaning no FD used whatsoever.

Table 2 Performance Statistics of the Algorithm Utilizing either AUP or BUP.

Algorithm		UWB Antenna				Compact RRC			
		Cost[1]	Cost savings[2] [%]	Max $\|S_{11}\|$[3] [dB]	SD (max$\|S_{11}\|$)[4] [dB]	Cost[1]	Cost savings[2] [%]	BW[5] [GHz]	SD(BW)[6] [GHz]
Reference		111.2	–	−14.9	0.6	43.0	–	0.27	0.01
AUP		58.3	47.6	–13.7	1.3	21.0	51.2	0.20	0.10
BUP β_0	0[$]	26.5	76.2	−13.3	1.7	15.9	63.0	0.18	0.11
	0.025	37.5	66.3	−13.9	1.3	13.4	68.8	0.20	0.06
	0.05	47.9	56.9	−14.0	0.9	28.9	32.8	0.23	0.04
	0.1	58.4	47.5	−13.7	1.1	27.0	37.2	0.22	0.05
	0.2	75.9	31.7	−14.3	0.9	42.6	0.9	0.22	0.05
	0.3	89.3	19.7	−14.2	0.8	41.3	4.0	0.21	0.06

[1] Number of EM simulations averaged over 10 algorithm runs (random initial points);
[2] Percentage-wise cost savings w.r.t. the reference algorithm;
[3] Objective function values for the UWB antenna (maximum in-band reflection S_{11} in dB);
[4] Standard deviation of S_{11} in dB across 10 algorithm runs;
[5] Objective function values for the compact RRC (bandwidth BW in GHz);
[6] Standard deviation of BW in dB across 10 algorithm runs;
[$] Broyden-only Jacobian updates meaning no FD used whatsoever.